Projected Climate Change Impacts on Water Demand and Supply for the City of Corvallis

July 2019

A Report to Carollo Engineers, Inc.

Prepared by
The Oregon Climate Change Research Institute

OCCRI

Projected Climate Change Impacts on Water Demand and Supply for the City of Corvallis, Oregon

A report to Carollo Engineers, Inc.

Prepared by David E. Rupp, PhD., Assistant Professor Senior Research

Reviewed by Peter Ruggiero, Ph.D., Interim Director
Editing and layout: Susan K. Osredker

Oregon Climate Change Research Institute
College of Earth, Ocean, and Atmospheric Sciences
104 CEOAS Admin Building
Oregon State University
Corvallis, OR 97331

July 2019

Cover image by Gary Braasch.

Recommended citation:
Rupp, D. E. (2019). Projected Climate Change Impacts on Water Demand and Supply for the City of Corvallis, Oregon: Report to Carollo Engineers, Inc. Oregon Climate Research Institute, Corvallis, OR.

Table of Contents

Executive Summary

This report provides an estimate of the impacts of climate change on factors affecting City of Corvallis (Corvallis) water demand and its primary water supply sources: the Willamette River and Rock Creek. The key climate-related changes (considered in isolation from other changes) are summarized below:

- ⇒ Projected higher summer temperatures and lower summer rainfall would increase water demand due to higher evaporative demand and desire for comfort during summer. Using irrigation of lawns as an example, approximately an additional 2 inches of water per unit area each summer may be necessary within 30 years, relative to a 1970-1999 baseline, if averaging over the available climate projections.
- ⇒ While flood magnitudes on the Willamette River are projected to increase, summer low flows are projected to decrease.

Both of these projected changes increase the risk of disruption of water supply from the Willamette River and increase the reliance on the management of upstream reservoirs to regulate flows for flood risk management during the wet season and to maintain sufficient supply for all needs (instream and consumptive) during the dry season. Little change is projected in annual water supply from Rock Creek, but future reductions in late spring flow may lead to a shorter time window of availability for water withdrawal.

Despite the critical importance of the quality of Corvallis' water sources, the varying pathways through which climate change can influence harmful algal blooms (HABs) in the Willamette Valley have not been well quantified, though most projected changes (higher temperatures; higher erosion rates from more intense precipitation and large wildfires, and the associated increased nutrient loading in Oregon's surface waters) point to a higher frequency of HABs. In addition to the impacts on water ***quantity***, one additional conclusion of this report is that there exists a large gap in knowledge of the degree to which climate change will impact the ***quality*** of the sources of water upon which Corvallis, and other communities in the Willamette Basin, rely.

Background: Regional climate change and its hydrological impacts

Since the beginning of the 20th century, the mean annual air temperature in the Pacific Northwest (PNW) has risen by 1.1° to 1.4° F (Abatzoglou et al., 2014a). This rise can be attributed primarily to the heating effects of anthropogenic greenhouse gas (GHG) emissions. Though other factors, such as solar variability, volcanic aerosol emissions, and natural variability in the circulation of the ocean and atmosphere, influence the region's climate, trends in these factors have been inconsistent with the century-long observed warming trend (Abatzoglou et al., 2014a; 2014b).

As GHG concentrations continue to increase (a certainty for the foreseeable future), temperatures are projected to continue increasing, with natural variability dampening or amplifying the rate of heating over multi-year to multi-decade time periods. Projections of future climate using global climate models (GCMs) indicate increases in annual temperature ranging from 2° to as much as 8° F for the PNW by the 2050s (Rupp et al., 2017a). (Note: Any changes reported here are relative to a 1970-1999 baseline unless otherwise indicated). This wide range in projected temperature increases has two principal causes. The first is that this range includes projections from two different scenarios of GHG accumulation in the atmosphere: One scenario represents a moderate effort to reduce global GHG emissions and the other represents a "business-as-usual" continuation of rising emissions throughout the 21st century. These scenarios are known as the Representative Concentration Pathways (RCPs) 4.5 and 8.5 respectively (Van Vuuren et al., 2011). The second reason for the large range is the differences among GCMs in how they simulate the region's temperature response to increasing GHGs, i.e., the GCMs show different *sensitivity* to changes in GHGs (Rupp et al., 2017a).

In the Willamette Valley, projected rates of heating are lower than in the PNW overall (Rupp et al., 2017b). This is due to the Valley's proximity to the Pacific Ocean which has a moderating effect on the heating, particularly in summer when inland temperatures show a much larger temperature increase than ocean temperatures. In summer, projected increases in temperatures in the Willamette Valley may be roughly 75% of those of the PNW-wide average increases.

Higher temperatures at the Earth's surface and in the lower atmosphere (i.e., the troposphere) influence precipitation by both permitting more water to be present in the atmosphere and by altering atmospheric circulation patterns. For the PNW, long-term changes in seasonal precipitation have not been observed except in spring where precipitation has shown an increasing trend. Though an increase is consistent with expectations given the higher observed temperatures, it is not known how much of this change can be attributed to anthropogenic causes (Abatzoglou et al., 2014a). No clear increases have been observed in extreme precipitation intensity in the PNW, unlike in other regions of the US (USGCRP, 2017).

Though the influence of a warmer global climate on precipitation has not be detected in the observational record of the PNW, climate projections from a large number of GCM simulations indicate changes in total annual precipitation ranging from -3% to +13% in PNW by the 2050s, depending on assumed GHG concentrations and particular GCM (Rupp et al., 2017a). These projections vary seasonally, with winter changes of -3% to +21% and summer changes of -28 to +11%. Natural variability is expected to be the largest contributor to near-term precipitation patterns for the next several decades, as evidenced by the lack of historical trends (Abatzoglou et al., 2014a) and projections that span both negative and positive changes indicating a large magnitude of natural variability relative to the anthropogenic impacts (Rupp et al., 2017a).

If even the average of these projected changes in temperature and precipitation are realized, they will have profound hydrological impacts in the region, as succinctly summarized in the 3rd Annual Oregon Climate Assessment (Dalton et al., 2017):

> *"Warming temperatures, changes in precipitation, and decreasing snowpack are already having, and will continue to have, significant impacts on hydrology and water resources in Oregon. Changes in the amount and seasonal timing of water in rivers and streams, changes in winter flood risk, and changes in summer extreme low flows are expected under future climate change. These hydrologic impacts will vary across watersheds. Watersheds that accumulate winter snowpack are most vulnerable to earlier peak streamflow timing. Watersheds with winter temperatures near the freezing level, such as intermediate to low elevations in the Oregon Cascades are particularly vulnerable. Projected future changes in water supply and demand are expected to strain the ability of existing infrastructure and operations to meet the many and varied water needs of Oregonians. In addition, changes in streamflow timing and amount and warming streams are expected to degrade freshwater fish habitat."*

For example, on the mainstem Willamette River, the magnitude of a flood with a 1% probability of being exceeded annually (i.e., the 100-year return period flood) has been projected to increase by roughly 20% (Tohver et al., 2014), taking the average of the projected hydrological changes. In contrast, average summer flows have been projected to decrease by 2% to 43% by the 2050s (Vano et al., 2015), with decreases of up to 50% in the average 7-day low flow (Tohver et al., 2014). All of these changes assume a river basin without reservoir management and water withdrawals (in other words, "natural" flows), so these projections indicate a greater future reliance on water systems to provide both flood risk management and year-round water access for human use.

Despite the large projected decreases in natural summer flows, a recent study of future water availability, use, and management in the Willamette Valley suggests a capacity to meet demand and minimum environmental flow requirements in the Willamette River throughout the 21st century, except for during drought years (Jaeger et al., 2017a; b).

These projections, made under the project known as Willamette Water 2100 (WW2100), consider the effects of the reservoirs, agriculture and municipal water use, and water rights. Built into these projections are assumptions about population growth, land use change, changes in water pricing, and improvements in water use efficiency.

The mainstem Willamette River gets most of its water from watersheds with historically significant snowpack - those identified as most vulnerable in the quoted passage above because of the large projected losses of snowpack in Cascades watersheds (e.g., Gergel et al., 2017; Jaeger et al. 2017). However, the City of Corvallis obtains a sizable fraction of its water from a Coast Range watershed with relatively little snowpack accumulation. It is expected that hydrological changes in Coast Range watersheds will be driven more by the intensification of the region's seasonal cycle (wetter wet winters and drier dry summers) and increased evapotranspiration during the warmer and longer growing season than by depletion of the snowpack. In the Marys River Watershed, previously published projections have winter runoff increasing by 0 to 6% while the mean annual 7-day low flow decreases by 5 to 10% by the 2040s (Chang and Jung, 2010; Jung and Chang, 2011; changes are relative to a 1960-1989 reference). Though these studies showed summer flows decreasing on average, the frequency of longer-duration hydrological droughts (6 to 24-month) were not projected to increase (Jung and Chang, 2012).

Beyond affecting the quantity and timing of freshwater supplies, climate change may have detrimental effects on the water quality by making environmental conditions more favorable for harmful algal blooms (HABs) that can contaminate drinking water sources with cyanobacteria that are natural toxins for humans and animals. HABs are already common in the Willamette Basin and have been observed in nearly all its major reservoirs (Schaedel, 2011, Appendix B; Carpenter, 2019), but the outbreak of cyanobacteria in the summer of 2018 that disrupted the drinking water supply to Salem, OR, raised public awareness and the level of concern. Higher air temperatures in the future will lead to higher temperature in local water supplies (e.g., Buccola et al., 2016) with water temperatures rising above thresholds that promote HABs; favorable HAB temperatures will also expand farther into spring and fall and into higher latitudes and elevations (USGRCP, 2016).

Higher temperature alone does not increase the likelihood of HABs; changes such as the stratification of the water column, higher pH (lower acidity), inputs of nutrients such as phosphorous (P), and the occurrence of previous HABs (Graham et al., 2016) also influence HAB likelihood. More intense precipitation causing more runoff and flooding has also been linked to HABs (USGCRP, 2016). In Willamette reservoirs, HABs may become more frequent as increased rainfall intensities lead to increasing erosion of the P-rich soils in the High Cascades. With the projected increase in the likelihood of wildfires in the Cascades (Mote et al., 2019) and the resulting loss in protective vegetation cover, the potential for

more erosion – and, in turn, more nutrient loading - also increases. In contrast to these factors promoting HABs, higher carbon dioxide (CO_2) in the atmosphere (the primary anthropogenic GHG) may lower water pH, making conditions *less* favorable for HABs (USGRCP, 2016), though it has been suggested that increased atmospheric CO_2 concentrations could stimulate the development of HABs in eutrophic waters by increasing the CO_2 concentration gradient at the water-air interface (Visser et al., 2016).

Because cyanobacteria form a very diverse group of organisms, there is no one set of environmental conditions that determines the population dynamics for all cyanobacteria (Huisman and Hulot, 2005). Though complex algorithms have been developed to help determine if conditions are favorable for particular genera (e.g., see flow chart in Oliver and Ganf, 2000, reprinted in Schaedel, 2011, Appendix A), it is still very challenging to predict HABs and to project the change in their frequency and extent into the future.

What follows in this report is a quantitative estimate of the impacts of climate change on factors affecting water demand and supply for the City of Corvallis, OR. Impacts to water quality in terms of toxicity from HABs, beyond the qualitative discussion given above, are not quantified as projections do not exist at this time.

Climate Change Impacts on Corvallis' Water Demand

Daily water demand is influenced by the weather, which drives both actual irrigation requirements and people's perception of watering needs and their desire for comfort (GSI, 2012). In general, annual maximum daily demand increases with higher maximum summer temperatures and with the number of consecutive days at high temperatures. The timing of the highest temperatures can also be a factor because customers may be more inclined to maintain a green lawn earlier in the summer than later. Low summer rainfall and a high number of consecutive days without rainfall also increase demand.

To assess the impact of climate change on water demand in Corvallis, changes over time in the following five meteorological variables were calculated:

- ⇒ Seasonal air temperature
- ⇒ Annual maximum air temperature
- ⇒ Seasonal evaporative demand
- ⇒ Seasonal precipitation
- ⇒ Annual maximum daily precipitation

Changes in these variables were based on climate projections for Corvallis under two scenarios of GHG and pollutant concentrations. These scenarios are defined by RCP4.5 and 8.5, the two most commonly used future emissions pathways. Two other RCPs exist (2.6

and 6.0) but the datasets being used for this study data are not available for these scenarios. Moreover, the ambitious RCP2.6 appears very unlikely to be realized. Under this high mitigation pathway, it could be possible to limit global warming to 2°C in line with the 2015 Paris agreement (UNFCCC, 2015), but net global emissions would need to be negative by 2100.

To characterize evaporative demand, we used potential evapotranspiration (PET) calculated using the standard Food and Agriculture Organization of the United Nations (FAO) method (see Appendix A).

Projections of seasonal and annual values of average daily temperature, maximum daily temperature, PET, and precipitation are given in Tables 1 through 4. Projections of precipitation minus potential evapotranspiration (P – PET) are also given in Table 5. P – PET, or atmospheric water supply minus demand, provides an index of the state of drought (e.g., McCabe and Wolock, 2015). Note that summers in Corvallis are characterized as being in a strong drought (P – PET is highly negative). Table 6 gives projections of annual maximum daily maximum temperature and annual maximum daily precipitation. All variables are given as averages of 20 climate simulations from 20 GCMs (see Appendix A) and as decadal averages for the 2020's (2020-2029) to the 2060's (2060-2069). Also given are baseline values averaged over the reference period 1970-1999.

Figures 1-5 show climate projections for the variables in the bulleted list above, except limited to the summer season (when demand is high) and annual extremes. These figures display the variables as smoothed time series for the years 1950-2099. Average summer daily maximum temperature is projected to increase by 5° F (RCP4.5) or 6° F (RCP8.5) by the 2050s, with average annual maximum daily maximum temperature reaching 103° F (RCP4.5) or 104° F (RCP8.5), compared to 98° F during the reference period. The maximum daily maximum temperature reaching 113° F in a given year during the 2050s would be considered within natural variability (i.e., not a freak occurrence) based on these projections (the current record is 108° F). Projected average summer precipitation decreases by about 1 inch by 2050.

This increase in temperature combined with a decrease in summer precipitation increases the drought index (P – PET), a measure of the evaporative demand not met by precipitation. The projected changes in P – PET by the 2050s imply that an additional 2.3 inches (RCP4.5) or 2.9 inches (RCP8.5) of water will be required to maintain a well-watered and green lawn during the summer months of June-August.

Table 1. Average winter (Dec.-Feb.), spring (Mar.-May), summer (Jun.-Aug.), fall (Sep.-Nov.), and annual temperature (°F) for a baseline period (1970-1999) and for the forthcoming 5 decades under RCP4.5 and RCP8.5, average of 20 simulations.

		Time period					
Season	RCP	1970-1999	2020-2029	2030-2039	2040-2049	2050-2059	2060-2069
Winter	4.5	40.8	42.3	42.9	43.5	44.2	44.7
	8.5	40.8	42.6	43.2	43.9	44.9	46.2
Spring	4.5	50.3	52.0	52.3	52.9	53.5	53.9
	8.5	50.3	52.1	52.6	53.3	54.1	55.1
Summer	4.5	64.5	66.4	67.1	67.8	68.8	69.4
	8.5	64.5	66.5	67.4	68.6	70.0	71.5
Fall	4.5	53.8	55.3	56.0	56.5	57.2	57.7
	8.5	53.8	55.4	56.2	57.4	58.6	59.8
Annual	4.5	52.3	54.0	54.5	55.2	55.9	56.4
	8.5	52.3	54.2	54.9	55.8	56.9	58.2

Table 2. Average winter (Dec.-Feb.), spring (Mar.-May), summer (Jun.-Aug.), fall (Sep.-Nov.), and annual daily maximum temperature (°F) for a baseline period (1970-1999) and for the forthcoming 5 decades under RCP4.5 and RCP8.5, average of 20 simulations.

		Time period					
Season	RCP	1970-1999	2020-2029	2030-2039	2040-2049	2050-2059	2060-2069
Winter	4.5	47.4	48.9	49.5	50.1	50.9	51.4
	8.5	47.4	49.1	49.8	50.6	51.5	52.9
Spring	4.5	60.5	62.3	62.6	63.2	63.8	64.2
	8.5	60.5	62.5	62.8	63.6	64.5	65.4
Summer	4.5	78.6	80.7	81.4	82.2	83.3	84.0
	8.5	78.6	80.8	81.7	83.0	84.6	86.1
Fall	4.5	64.7	66.3	67.0	67.6	68.2	68.7
	8.5	64.7	66.5	67.3	68.5	69.8	70.9
Annual	4.5	62.8	64.6	65.1	65.8	66.5	67.1
	8.5	62.8	64.7	65.4	66.4	67.6	68.8

Table 3. Winter (Dec.-Feb.), spring (Mar.-May), summer (Jun.-Aug.), fall (Sep.-Nov.), and annual potential evapotranspiration (inches) for a baseline period (1970-1999) and for the forthcoming 5 decades under RCP4.5 and RCP8.5, average of 20 simulations.

		Time period					
Season	RCP	1970-1999	2020-2029	2030-2039	2040-2049	2050-2059	2060-2069
Winter	4.5	2.7	2.8	2.9	2.9	3.0	3.0
	8.5	2.7	2.8	2.9	2.9	3.0	3.1
Spring	4.5	9.7	10.1	10.1	10.3	10.4	10.6
	8.5	9.7	10.2	10.2	10.3	10.5	10.7
Summer	4.5	17.4	18.3	18.5	18.8	19.1	19.4
	8.5	17.4	18.5	18.8	19.1	19.7	20.0
Fall	4.5	7.8	8.1	8.2	8.3	8.5	8.5
	8.5	7.8	8.2	8.3	8.5	8.8	8.9
Annual	4.5	37.6	39.3	39.8	40.3	41.0	41.5
	8.5	37.6	39.7	40.1	40.9	42.0	42.8

Table 4. Winter (Dec.-Feb.), spring (Mar.-May), summer (Jun.-Aug.), fall (Sep.-Nov.), and annual precipitation (inches) for a baseline period (1970-1999) and for the forthcoming 5 decades under RCP4.5 and RCP8.5, average of 20 simulations.

		Time period					
Season	RCP	1970-1999	2020-2029	2030-2039	2040-2049	2050-2059	2060-2069
Winter	4.5	19.6	19.6	19.9	19.8	20.5	20.9
	8.5	19.6	20.1	19.8	20.2	20.6	20.7
Spring	4.5	9.3	9.2	9.1	9.2	9.1	8.9
	8.5	9.3	8.9	9.2	9.4	9.2	9.2
Summer	4.5	2.5	2.1	2.1	2.0	1.9	1.9
	8.5	2.5	2.0	2.0	2.0	1.9	1.9
Fall	4.5	11.5	11.2	11.4	11.5	11.2	11.2
	8.5	11.5	10.9	11.0	11.1	11.0	11.3
Annual	4.5	42.9	42.1	42.6	42.5	42.8	42.9
	8.5	42.9	42	41.9	42.7	42.7	43.0

Table 5. Average winter (Dec.-Feb.), spring (Mar.-May), summer (Jun.-Aug.), fall (Sep.-Nov.), and annual precipitation minus potential evapotranspiration (P-PET; inches) for a baseline period (1970-1999) and for the forthcoming 5 decades under RCP4.5 and RCP8.5, average of 20 simulations.

		Time period					
Season	RCP	1970-1999	2020-2029	2030-2039	2040-2049	2050-2059	2060-2069
Winter	4.5	16.9	16.8	17.0	16.9	17.5	17.9
	8.5	16.9	17.3	16.9	17.3	17.6	17.6
Spring	4.5	-0.4	-0.9	-1.0	-1.1	-1.3	-1.7
	8.5	-0.4	-1.3	-1.0	-0.9	-1.3	-1.5
Summer	4.5	-14.9	-16.2	-16.4	-16.8	-17.2	-17.5
	8.5	-14.9	-16.5	-16.8	-17.1	-17.8	-18.1
Fall	4.5	3.7	3.1	3.2	3.2	2.7	2.7
	8.5	3.7	2.7	2.7	2.6	2.2	2.4
Annual	4.5	5.3	2.8	2.8	2.2	1.8	1.4
	8.5	5.3	2.3	1.8	1.8	0.7	0.2

Table 6. Average annual maximum daily maximum temperature and average annual maximum daily precipitation for a baseline period (1970-1999) and for the forthcoming 5 decades under RCP4.5 and RCP8.5, average of 20 simulations.

		Time period					
Variable	RCP	1970-1999	2020-2029	2030-2039	2040-2049	2050-2059	2060-2069
Ave. annual max. daily maximum temperature (°F)	4.5	98.0	99.6	100.3	101.6	102.8	103.2
	8.5	98.0	99.9	101.0	102.4	103.9	105.2
Ave. annual max. daily precipitation (inches)	4.5	2.1	2.2	2.2	2.2	2.2	2.3
	8.5	2.1	2.1	2.2	2.3	2.3	2.3

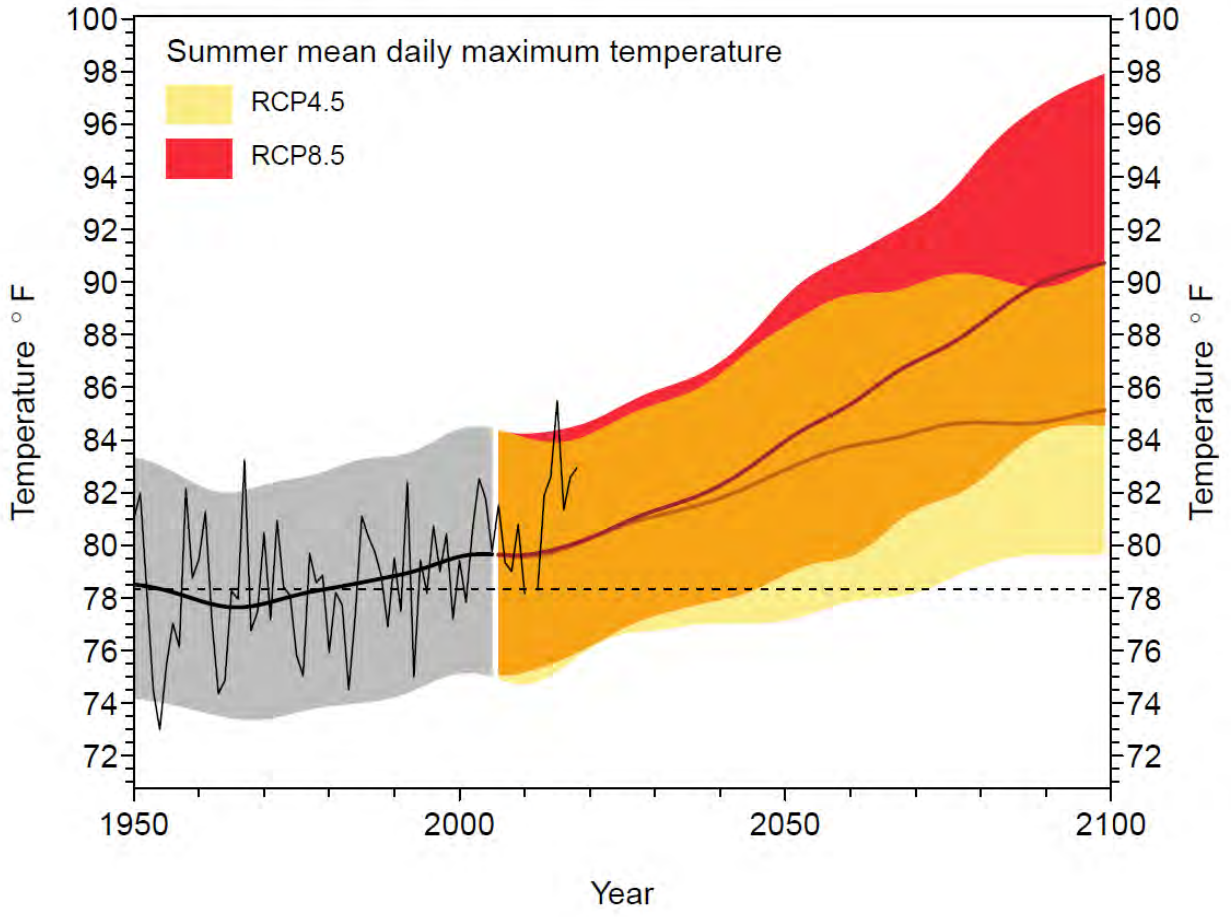

Figure 1. Summer (Jun.-Aug.) average daily maximum temperature for Corvallis, 1950-2099. Shown are the observed historical (1950-2018; thin black line) and simulated historical and projected values under a lower (RCP 4.5) and a higher (RCP 8.5) future emissions scenario. The thicker black line depicts the mean values of simulations from 20 climate models for the 1950-2005 period based on observed climate drivers (i.e., anthropogenic greenhouse gases and pollutants and natural drivers such as volcanic emissions and variable solar output). The orange and red lines depict the 20-model average for the 2006-2099 period for the two future scenarios (dark orange = RCP4.5, red = RCP8.5). The shading depicts the range in annual temperatures from all 20 models (yellow = RCP4.5, red = RCP8.5, orange = overlap). The time series of the 20-model mean and range have been smoothed to emphasize the long-term trend over short-term (e.g., year-to-year) variability. The horizontal dashed line indicates the average simulated value over the years 1950-1999.

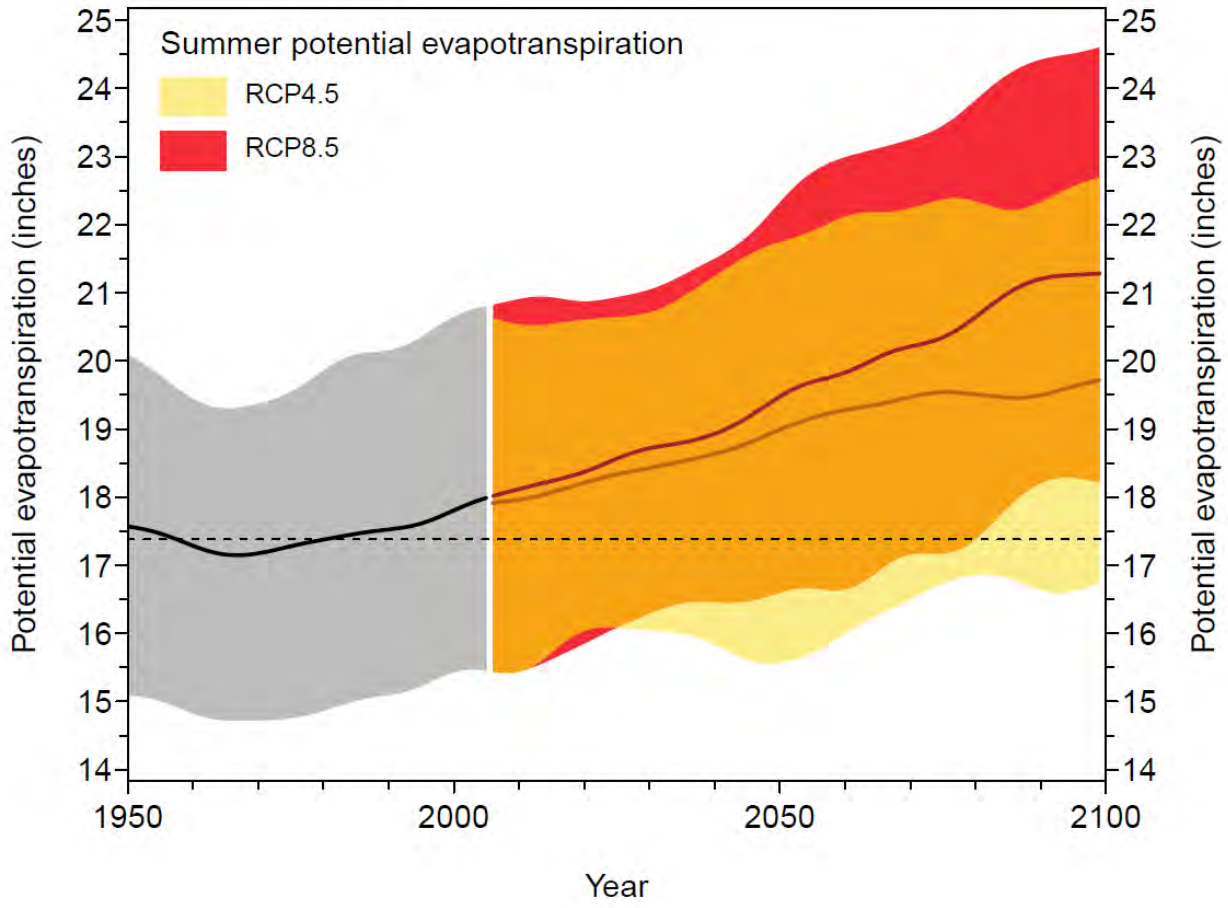

Figure 2. Total summer (Jun.-Aug.) potential evapotranspiration for Corvallis, 1950-2099. Shown are the observed historical (1950-2018; thin black line) and simulated historical and projected values under a lower (RCP 4.5) and a higher (RCP 8.5) future emissions scenario. The thicker black line depicts the mean values of simulations from 20 climate models for the 1950-2005 period based on observed climate drivers (i.e., anthropogenic greenhouse gases and pollutants and natural drivers such as volcanic emissions and variable solar output). The orange and red lines depict the 20-model average for the 2006-2099 period for the two future scenarios (dark orange = RCP4.5, red = RCP8.5). The shading depicts the range in annual temperatures from all 20 models (yellow = RCP4.5, red = RCP8.5, orange = overlap). The time series of the 20-model mean and range have been smoothed to emphasize the long-term trend over short-term (e.g., year-to-year) variability. The horizontal dashed line indicates the average simulated value over the years 1950-1999.

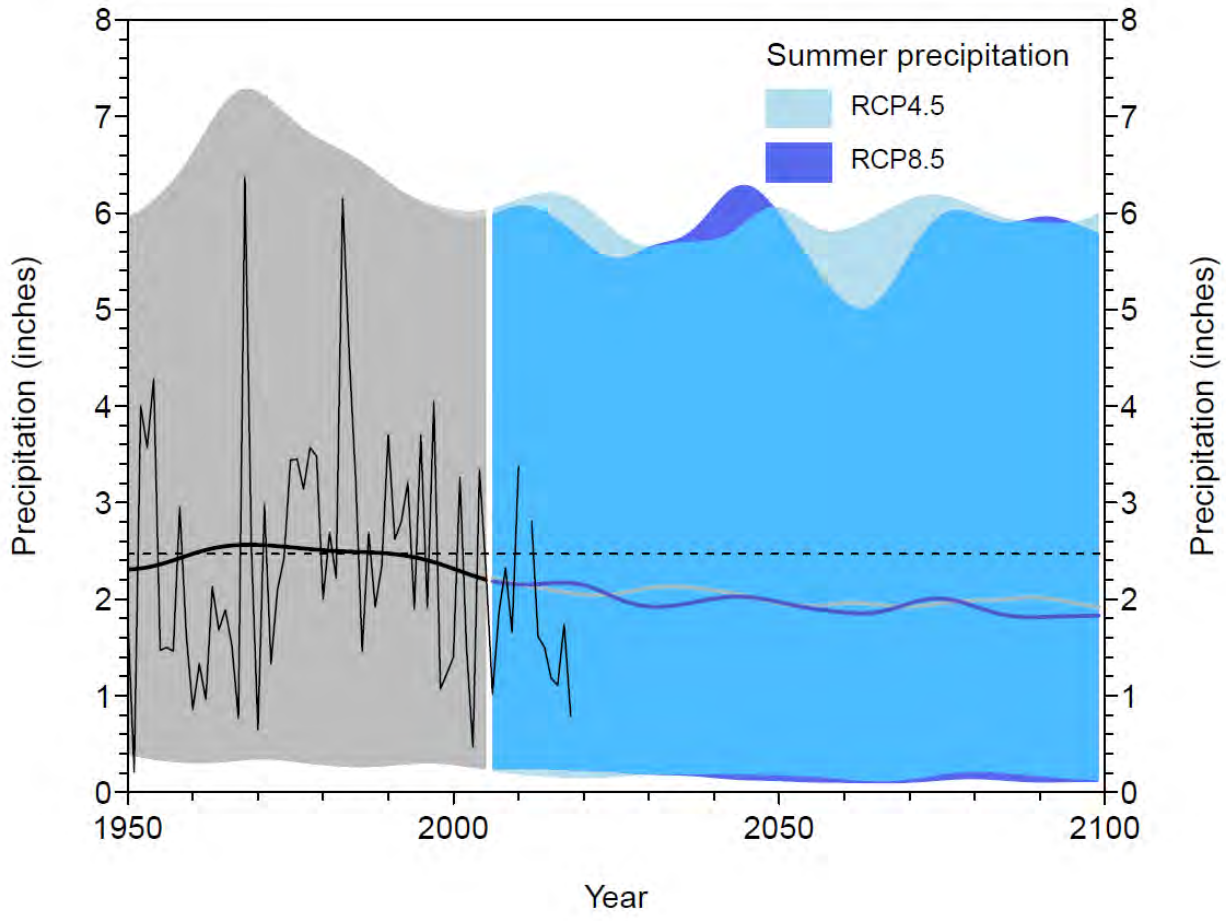

Figure 3. Total summer (Jun.-Aug.) precipitation for Corvallis, 1950-2099. Shown are the observed historical (1950-2018; thin black line) and simulated historical and projected values under a lower (RCP 4.5) and a higher (RCP 8.5) future emissions scenario. The thicker black line depicts the mean values of simulations from 20 climate models for the 1950-2005 period based on observed climate drivers (i.e., anthropogenic greenhouse gases and pollutants and natural drivers such as volcanic emissions and variable solar output). The light and dark blue lines depict the 20-model average for the 2006-2099 period for the two future scenarios (light blue = RCP4.5, dark blue = RCP8.5). The shading depicts the range in annual temperatures from all 20 models (light blue = RCP4.5, dark blue = RCP8.5, medium blue = overlap). The time series of the 20-model mean and range have been smoothed to emphasize the long-term trend over short-term (e.g., year-to-year) variability. The horizontal dashed line indicates the average simulated value over the years 1950-1999.

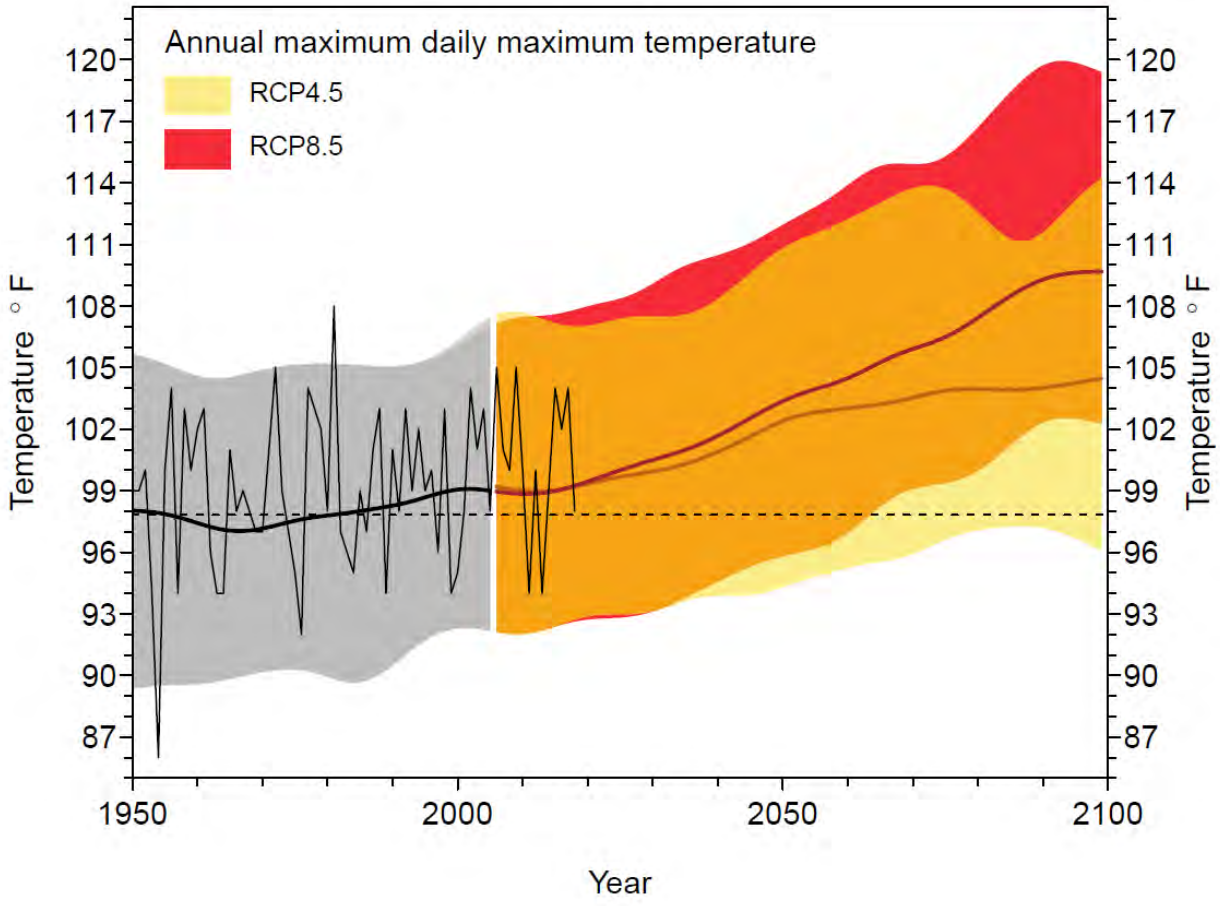

Figure 4. Annual maximum daily maximum temperature for Corvallis, 1950-2099. Shown are the observed historical (1950-2018; thin black line) and simulated historical and projected values under a lower (RCP 4.5) and a higher (RCP 8.5) future emissions scenario. The thicker black line depicts the mean values of simulations from 20 climate models for the 1950-2005 period based on observed climate drivers (i.e., anthropogenic greenhouse gases and pollutants and natural drivers such as volcanic emissions and variable solar output). The orange and red lines depict the 20-model average for the 2006-2099 period for the two future scenarios (dark orange = RCP4.5, red = RCP8.5). The shading depicts the range in annual temperatures from all 20 models (yellow = RCP4.5, red = RCP8.5, orange = overlap). The time series of the 20-model mean and range have been smoothed to emphasize the long-term trend over short-term (e.g., year-to-year) variability. The horizontal dashed line indicates the average simulated value over the years 1950-1999.

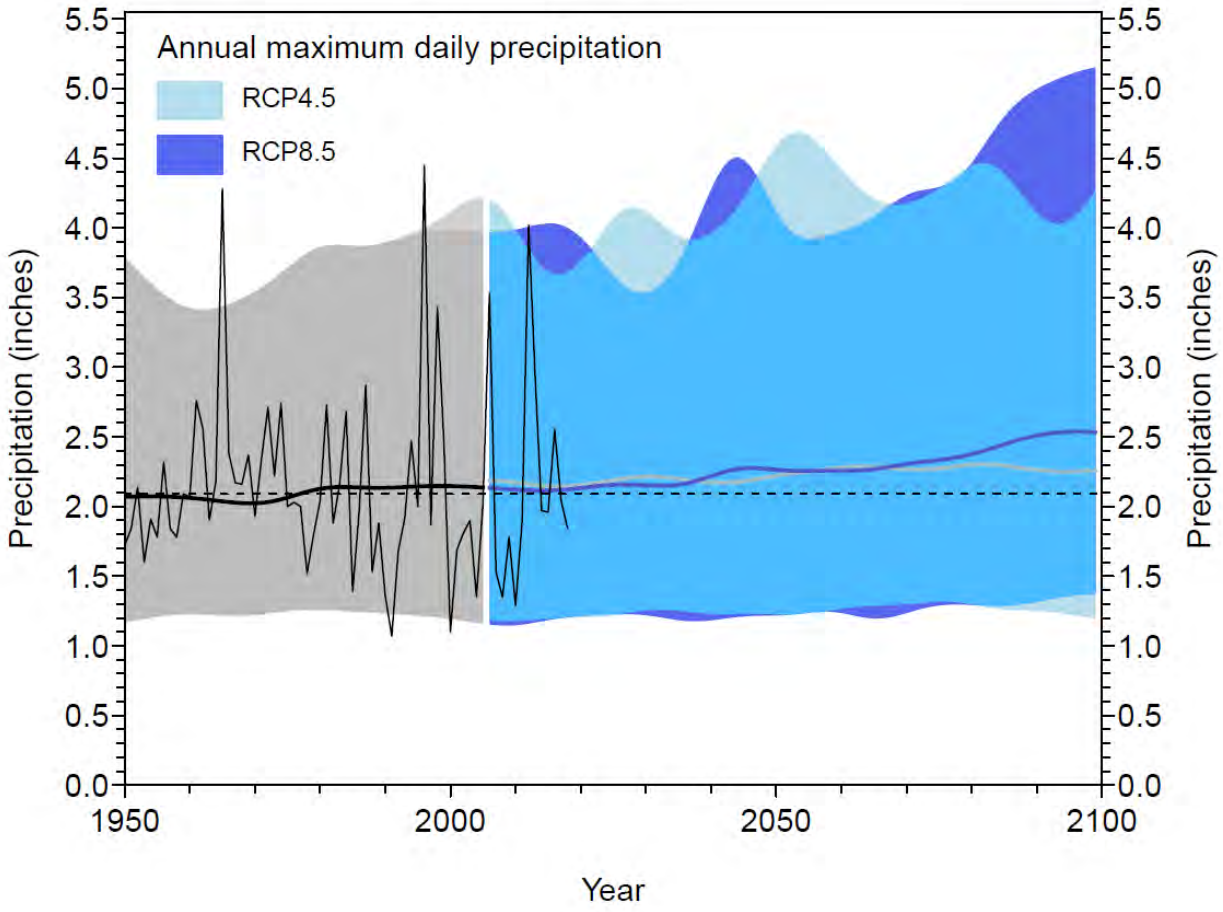

Figure 5. Annual maximum daily precipitation for Corvallis, 1950-2099. Shown are the observed historical (1950-2018; thin black line) and simulated historical and projected values under a lower (RCP 4.5) and a higher (RCP 8.5) future emissions scenario. The thicker black line depicts the mean values of simulations from 20 climate models for the 1950-2005 period based on observed climate drivers (i.e., anthropogenic greenhouse gases and pollutants and natural drivers such as volcanic emissions and variable solar output). The light and dark blue lines depict the 20-model average for the 2006-2099 period for the two future scenarios (light blue = RCP4.5, dark blue = RCP8.5). The shading depicts the range in annual temperatures from all 20 models (light blue = RCP4.5, dark blue = RCP8.5, medium blue = overlap). The time series of the 20-model mean and range have been smoothed to emphasize the long-term trend over short-term (e.g., year-to-year) variability. The horizontal dashed line indicates the average simulated value over the years 1950-1999.

Climate Change Impacts on Corvallis' Water Supply Availability

Corvallis gets its water from two sources: The Willamette River and Rock Creek, a tributary of the Marys River. This section explores how climate change over the next 50 years may change the risk of disruption to the Willamette River water supply from extremely high and extremely low flows and how climate change may affect the volume and timing of supply from Rock Creek.

Extremely high flows can disrupt service when the flood waters inundate infrastructure necessary for water treatment, as well as carry heavy sediment loads and water pollutants. In contrast, extreme drought could result in insufficient flow to meet the unconverted minimum perennial streamflow of 1750 cfs at the Albany gage, Corvallis' demand for water under water right permit S-35551, and all water rights above the Albany gage senior to Corvallis' permit. For extremely high flow, this study is limited to changes in flood flow magnitude and does not cover extent and depth of inundation which requires additional modeling and analysis. For extremely low flows, this study examines the frequency of flow falling below specified thresholds. The methods used to identify the low flow threshold on the Willamette River and how these low-flow changes would directly affect access to Willamette River water under potential changes to water policy and reservoir management has been assessed by GSI Water Solutions, Inc. and is reported in Chapter 5 of Corvallis' Water Distribution and Treatment Facilities Master Plan.

Willamette River

Change in flood risk was assessed by calculating the projected changes in the magnitude of Willamette River streamflow with a 4%, 1%, and 0.2% probability of being exceeded. These probabilities are equivalent to what are commonly referred to as the 25, 100, and 500-year return periods, respectively. 'Naturalized' streamflow, also known as no-regulation, no-irrigation (NRNI) streamflow, was used for this assessment. This NRNI streamflow is an estimate of what the streamflow would have been had there been no reservoir operations nor water used for irrigation upstream. Actual flood flows will be lower than NRNI flows and will depend on the actions taken by the reservoir operators to manage flood risk. However, it is plausible that a '500-year flood' could overwhelm the Willamette River reservoir system's capacity to reduce the peak flow by a consequential amount.

By considering relative changes in the magnitude of NRNI flood flows, we can still evaluate the changes in pressure on the reservoir system to manage flood risk for floods that do not overwhelm the system. Consider the recent flooding in Corvallis (April, 2019) that was reduced by the reservoir operations. Taking this to be roughly a 25-year return period

event, based on the observed flood record, we can calculate by how much the peak NRNI streamflow of this event may increase under climate change. In the worst case, all of this additional water would pass through the system unmodified.

Water supply risk was assessed by considering the unconverted minimum perennial streamflow at Albany and the consumptive use of all water rights senior to Corvallis' Willamette permit S-35551 upstream of the Albany gage. We considered water access to be at risk when NRNI streamflow drops below threshold values at Albany (2,285 cfs) and Salem (2,150 cfs) (GSI, personal communication). Under present-era reservoir operations, streamflow at Albany and Salem never drop to these levels because the natural flow is augmented by reservoir releases. However, changes in regulations may distinguish between 'natural' flow and reservoir releases which could affect how much of the actual river water Corvallis has legal access to at any given time.

Figs. 6 and 7 show two example water years of daily observed and NRNI streamflow at Albany and Salem, respectively. Water years 1965 and 1994 were chosen because they have the highest and lowest daily flows, respectively, in the NRNI record since 1950. From Fig. 8a, we can see that management reduced the peak daily flow of the December, 1964, flood, from just over 300 kcfs to under 200 kcfs at Albany, based on USACE's estimated NRNI flow. We can also see the results of operators' efforts to maintain the flow above 4 kcfs throughout the year at Albany, against the natural proclivity to drop below 2-3 kcfs from mid-summer until the onset of the wet season.

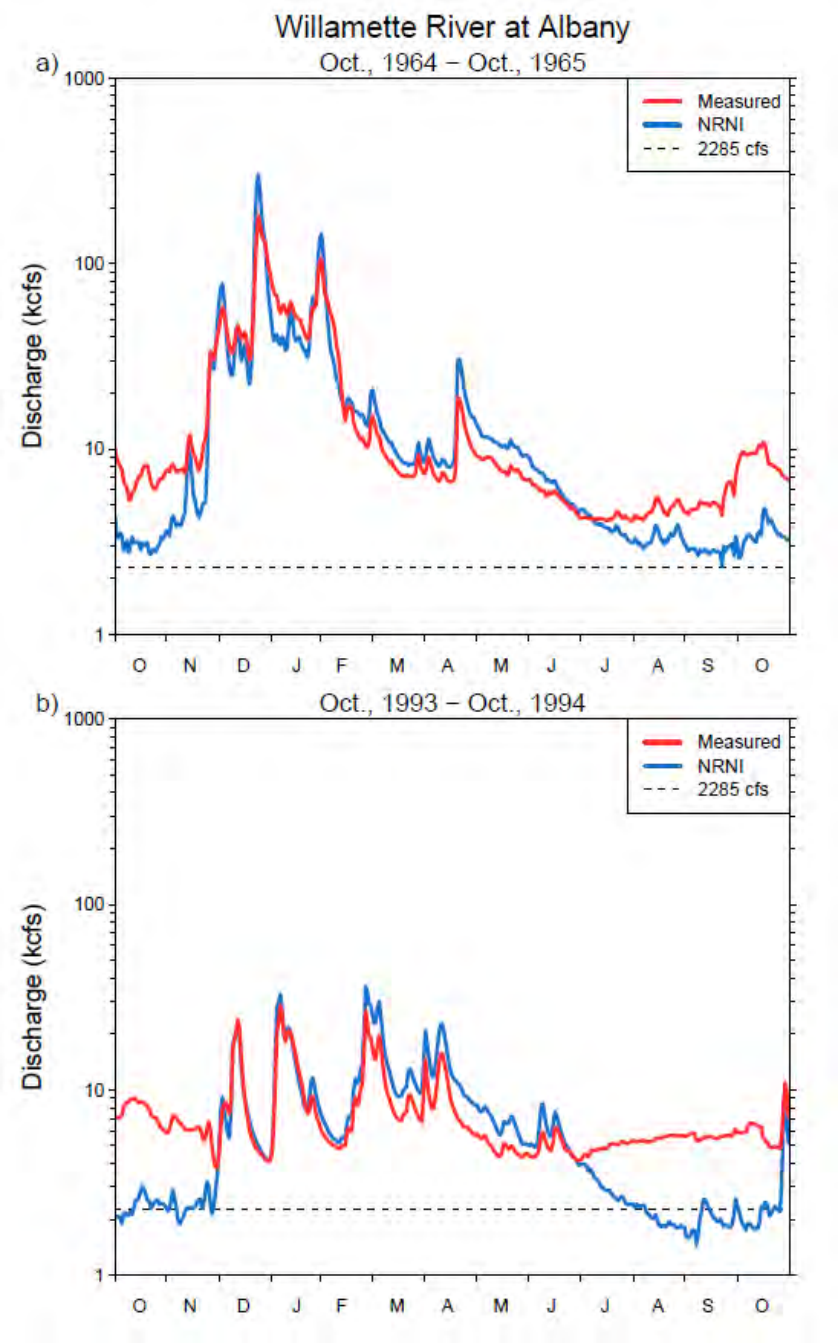

Figure 6. Measured and estimated no-regulation, no-irrigation (NRNI) daily discharge at the Willamette River at Albany for a) Oct. 1964 - Oct. 1965 and b) Oct. 1993 - Oct. 1994. The highest NRNI daily discharge since 1950 occurred Dec., 24, 1964 (301.5 kcfs) and the lowest occurred Sep. 7, 1994 (1.5 kcfs). Note the y-axis is logarithmic.

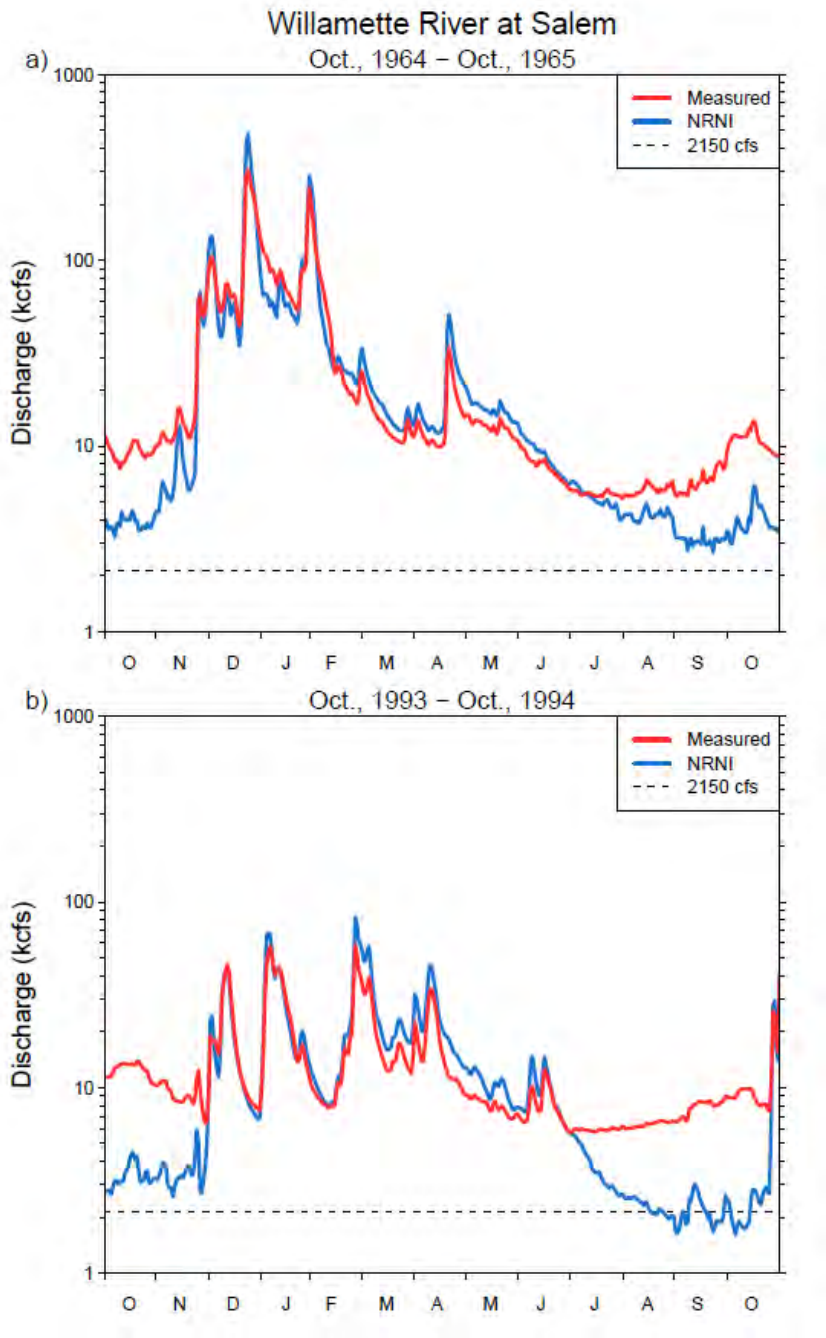

Figure 7. Measured and estimated no-regulation, no-irrigation (NRNI) daily discharge at the Willamette River at Salem for a) Oct. 1964 - Oct. 1965 and b) Oct. 1993 - Oct. 1994. The highest NRNI daily discharge since 1950 occurred Dec., 24, 1964 (478.7 kcfs) and the lowest occurred Oct. 6, 1994 (1.6 kcfs). Note the y-axis is logarithmic.

Willamette River - Flood Flows

Projected percentage change in NRNI annual (water year) maximum daily flow with 4%, 1%, and 0.2% probabilities of exceedance at the Willamette River at Albany are shown in Fig. 8. Changes are calculated for the period 2021-2070 relative to the period 1951-2000 for each of 160 hydrological simulations from the Columbia River Climate Change (CRCC) project (See Appendix B).

Overall trends are towards an increase in magnitude of flood flows, though the uncertainty in the underlying response to GHGs increases as the exceedance probabilities decrease. For the 4% exceedance probability, an overwhelming number (97.5%) of simulations show an increase streamflow. This percentage of simulations reduces to 85% and 75% for the 1% and 0.2% exceedance flows, respectively.

Individual simulations span very large ranges of changes (e.g., -40% to +275% for the 0.2% exceedance probability). A large proportion of this range is due simply to natural variability (the particular sequence of weather events generated by each GCM in each simulation) and the randomness inherent in sampling a particular 50-year period, while some is due to how sensitive each GCM is to increasing GHG concentrations. Results in Fig. 8 also reveal considerable dependency on the choice of hydrological model and the choice of downscaling method.

Without additional research that may lead to strong reasons to justify favoring any particular subset of GCMs, hydrological models, or downscaling method, the "best" estimate of the effect of increasing GHGs on flood flows can be made by averaging the changes over all the available simulations. In fact, selecting a subset of GCM simulations introduces its own problem, which is to increase our uncertainty in the hydrological response simply by reducing the sample size over which we average. The best estimates are given in Table 7. They indicate an increase in flood flow in the range of 20 to 30%, with larger increase for RCP8.5 than RCP4.5 and larger percent increases for the rarer floods.

It is worth noting that under a changing climate, the flood probabilities will not be constant over a 50-year period, yet the standard statistical method used here implicitly makes this assumption. When interpreting the statistical results, we should be aware that changes for the first years of 2021-2070 period would be smaller than those reported in Table 7 if probabilities were allowed to vary gradually year by year as GHG concentrations steadily increase. Likewise, changes for the years near the end of 2021-2070 would be greater than those reported.

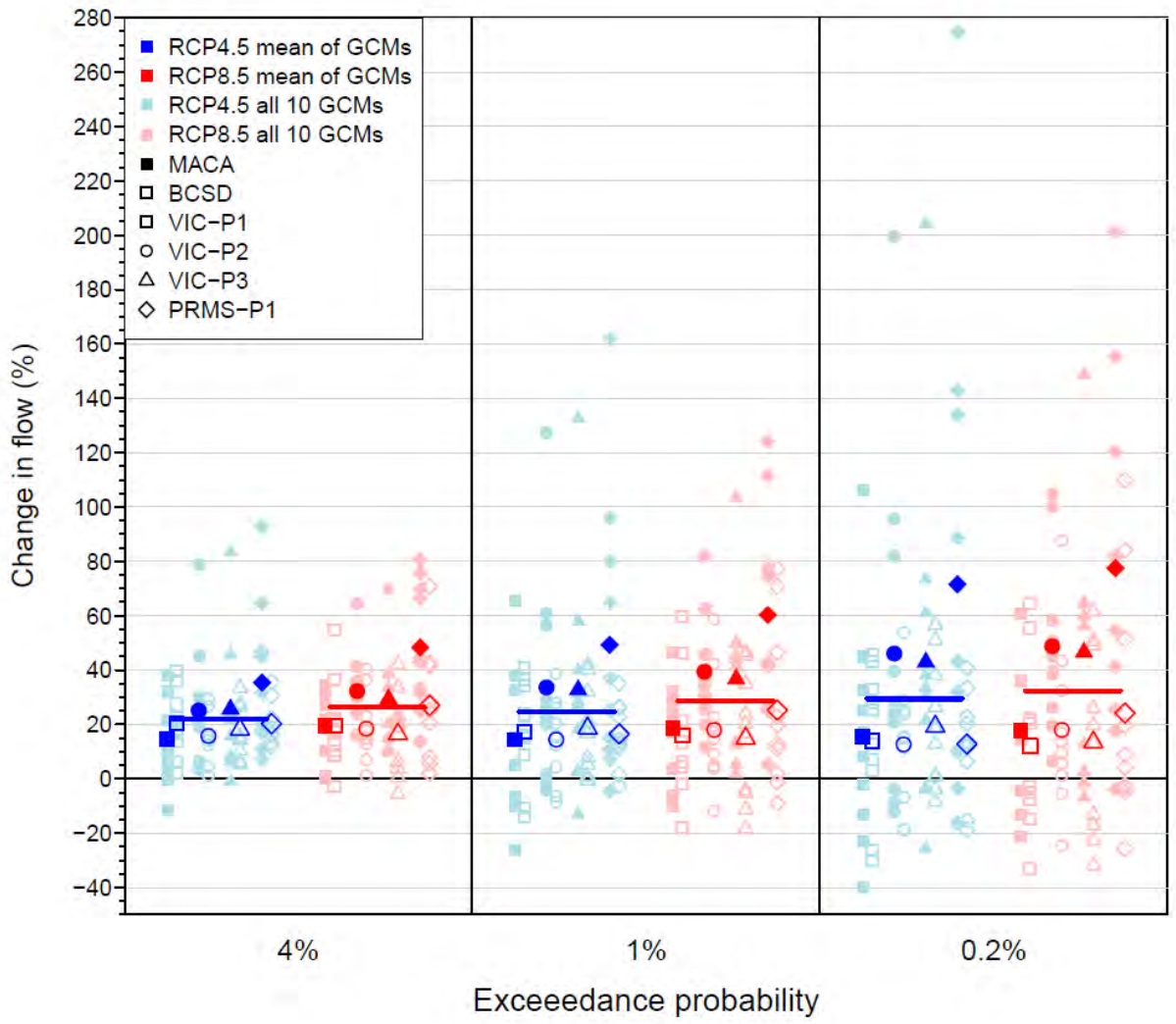

Figure 8. Projected relative change in NRNI annual (water year) maximum daily flow with 4%, 1%, and 0.2% probabilities of exceedance at the Willamette River at Albany. Changes are calculated for the period 2021-2070 relative to the period 1951-2000 for each of 160 hydrological simulations (see Appendix B). Blue and red horizontal line segments show the average for all simulations under RCP4.5 and RCP8.5, respectively (80 simulations per RCP), for each exceedance probability.

Table 7. Projected relative change (%) in NRNI annual (water year) maximum daily flow with 4%, 1%, and 0.2% probabilities of exceedance at the Willamette River at Albany. Changes are averaged over all 80 simulations within each RCP scenario.

Scenario	Exceedance probability		
	4%	1%	0.2%
RCP 4.5	+22	+25	+29
RCP 8.5	+26	+29	+32

Willamette River - Low Flows

The cumulative number of days that streamflow drops below threshold values at Albany (2,285 cfs) and Salem (2,150 cfs) since 1960 are shown Figs. 9 and 10, respectively. Fig. 9a and 10a show results from all 160 simulations, and Figs. 9b and 10b show only the average from all simulations. It is evident that daily natural streamflows below these thresholds would be a common occurrence. At Albany, the NRNI record shows an average rate of 20 days per year from 1980 to 2008 that the flow would have dropped below 2,285 cfs. The hydrological projections show these rates increasing to 30 days per year over the next three decades and 45 days per year from 2041-2070 for RCP4.5. For RCP8.5, these rates increase to 35 and 59 days per year, respectively. These values are calculated from averaging the results of all the simulations, but there is much variability among the individual simulations. In the most extreme cases, the rates for individual simulations are double the average rate.

At Salem there are many fewer days (roughly a third of number of days for Albany) that streamflow falls below the defined threshold, indicating the location of concern for the potential regulation of the City's Willamette River water rights is the Albany gage.

The average number of days that NRNI and CRCC streamflow falls below the defined thresholds at Albany and Salem have also been calculated for each month of the calendar year, averaged over the periods 1979-2008, 2011-2040, and 2041-2070, and over all simulations. These values are available in the Supporting Materials.

In the observed record, the flow has never dropped below the defined thresholds since 1960 at Albany nor at Salem. The two future hydrological scenarios from WW2100 also never simulate the regulated flow dropping below the defined thresholds at Albany nor Salem. This latter result suggests sufficient capacity in the reservoir system to cope with the projected changes in the natural flow regimes. According to the WW2100 study, it also reflects shifting agriculture water demand towards an earlier growing season that helps offset PET increases in late summer (Jaeger, 2017a). However, it should be noted that the WW2100 considered only two future hydrological scenarios, whereas the 160 CRCC simulations (Figs. 9a and 10a) suggest there is a very large range of plausible outcomes that were not considered by the WW2100 study.

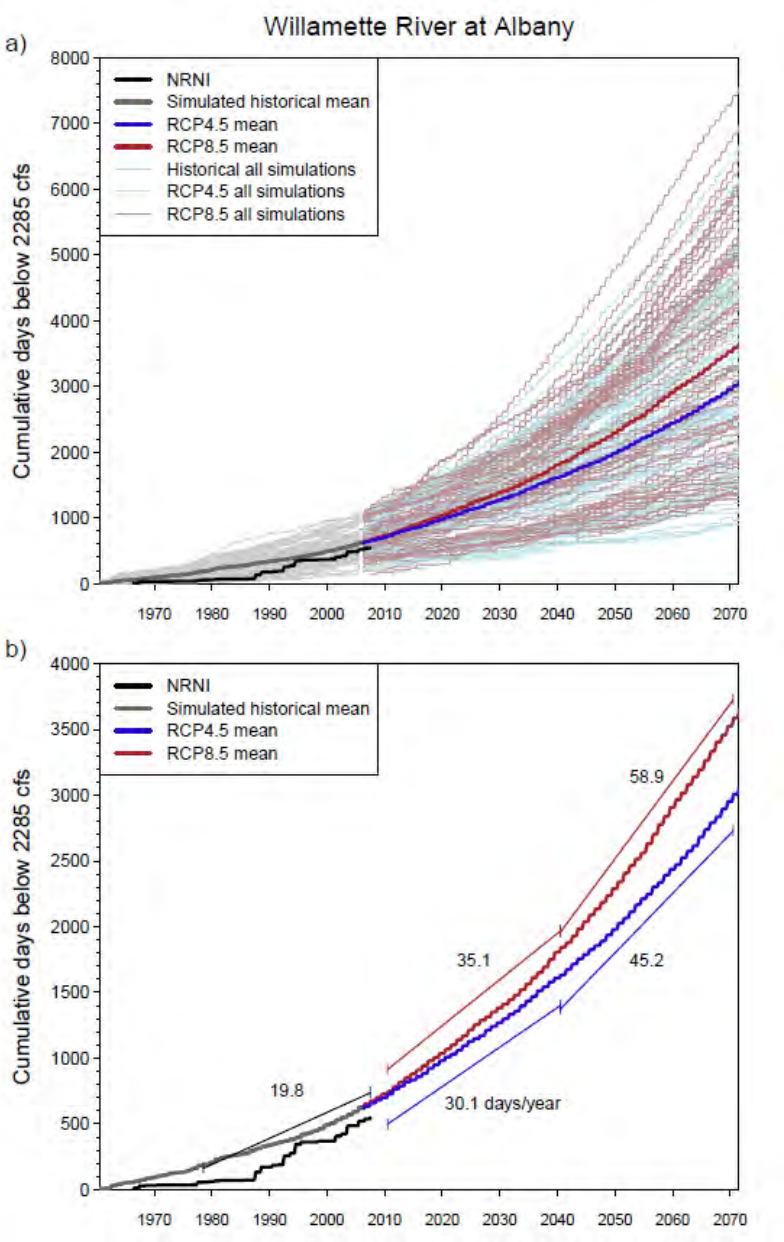

Figure 9. a) Cumulative number of days since Oct. 1, 1960, that discharge falls below 2,285 kcfs at the Willamette River at Albany in the no-regulation, no-irrigation (NRNI) record and in all 160 simulations from the CRCC project. Light gray lines denote simulations assuming historical greenhouse gas concentrations through 2005 and light blue and red lines denote simulations assuming greenhouse gas concentrations defined by the RCP4.5 and RCP8.5 scenarios, respectively. The darker gray, blue, and red lines show the average of all 160 simulations. b) Same as (a) but showing only the average of all 160 simulations. The numbers in (b) give the average number of days per year that the discharge drops below 2,285 kcfs over the period indicated by each line segment. Pre-2009 values are for the NRNI record and values after 2010 are for the RCP4.5 and RCP8.5 simulations.

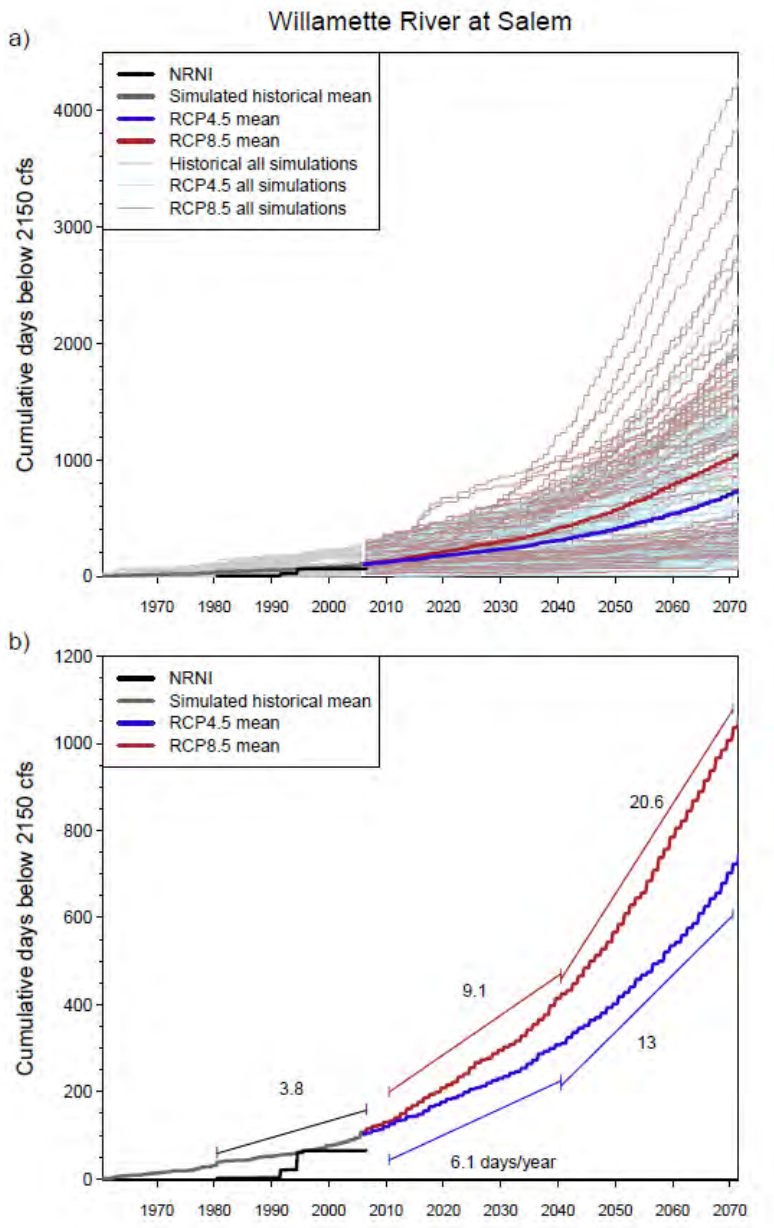

Figure 10. a) Cumulative number of days since Oct. 1, 1960, that discharge falls below 2,150 kcfs at the Willamette River at Salem in the no-regulation, no-irrigation (NRNI) record and in all 160 simulations from the CRCC project. Light gray lines denote simulations assuming historical greenhouse gas concentrations through 2005 and light blue and red lines denote simulations assuming greenhouse gas concentrations defined by the RCP4.5 and RCP8.5 scenarios, respectively. The darker gray, blue, and red lines show the average of all 160 simulations. The numbers in (b) give the average number of days per year that the discharge drops below 2,150 kcfs over the period indicated by each line segment. Pre-2009 values are for the NRNI record and values after 2010 are for the RCP4.5 and RCP8.5 simulations.

Rock Creek

Changes in water supply from Rock Creek were assessed by comparing long-term mean monthly streamflow for two future climate scenarios. The climate scenarios were the same as those used in the WW2100 study (MIROC5 RCP8.5 and HadGEM2-ES RCP8.5; see Appendix B). Statistics of extreme flow (high and low) were not analyzed because of the shortness of the observation record, and concerns about the ability of the hydrological model to accurately simulate extreme conditions in such a small watershed.

Simulated changes in the 30-year mean annual hydrograph over time are illustrated in Fig. 11. While there are multi-decadal fluctuations in the hydrograph due to natural variability, the long-term trend is toward increased flow in early winter (Nov.-Dec.) and decreased flow in spring and summer.

To reduce some the influence of natural variability, changes in 50-year means were calculated (1971-2020 and 2021-2070) and averaged over the two climate scenarios (Table 8). Projected decreases in flow from historical values are substantial in May (-43%) with flow nearly depleted by August (-96%), though at that time of year flow in Rock Creek is not a contributor to Corvallis' water supply. Still, the flow decreases in spring could mean a substantially reduced window of water access from Rock Creek during the year, without construction of storage facilities to offset declines.

The relative reductions in late spring and summer flow are large, but this could be in part due to the model's underestimation of streamflow during this period. Improvement in the model's ability to simulate summer flow would likely affect the reported changes, making the relative changes smaller if the simulated baseline period summer flows were increased. It is also worth noting that the simulated flows do not include the February peak that exists in the observations (Fig. 11). The observed peak in February either suggests an unusually rainy February during the years of streamflow measurements or that snow accumulation over the prior months of December and January is a more important part of the basin hydrology than was expected; if so, it points to deficiency in the hydrological model that could be the result of one or more factors: 1) errors in precipitation and/or temperature inputs; 2) an incorrect function in the model for determining when precipitation falls as snow; 3) a poorly performing snowpack model. However, if snow is an important factor, this would only imply that rising temperatures would result in yet larger hydrological impacts. Given the shortcomings of the model, the reported values should be used more qualitatively than quantitatively, i.e., the City should be prepared for a reduction in average spring and summer flow as a distinct possibility.

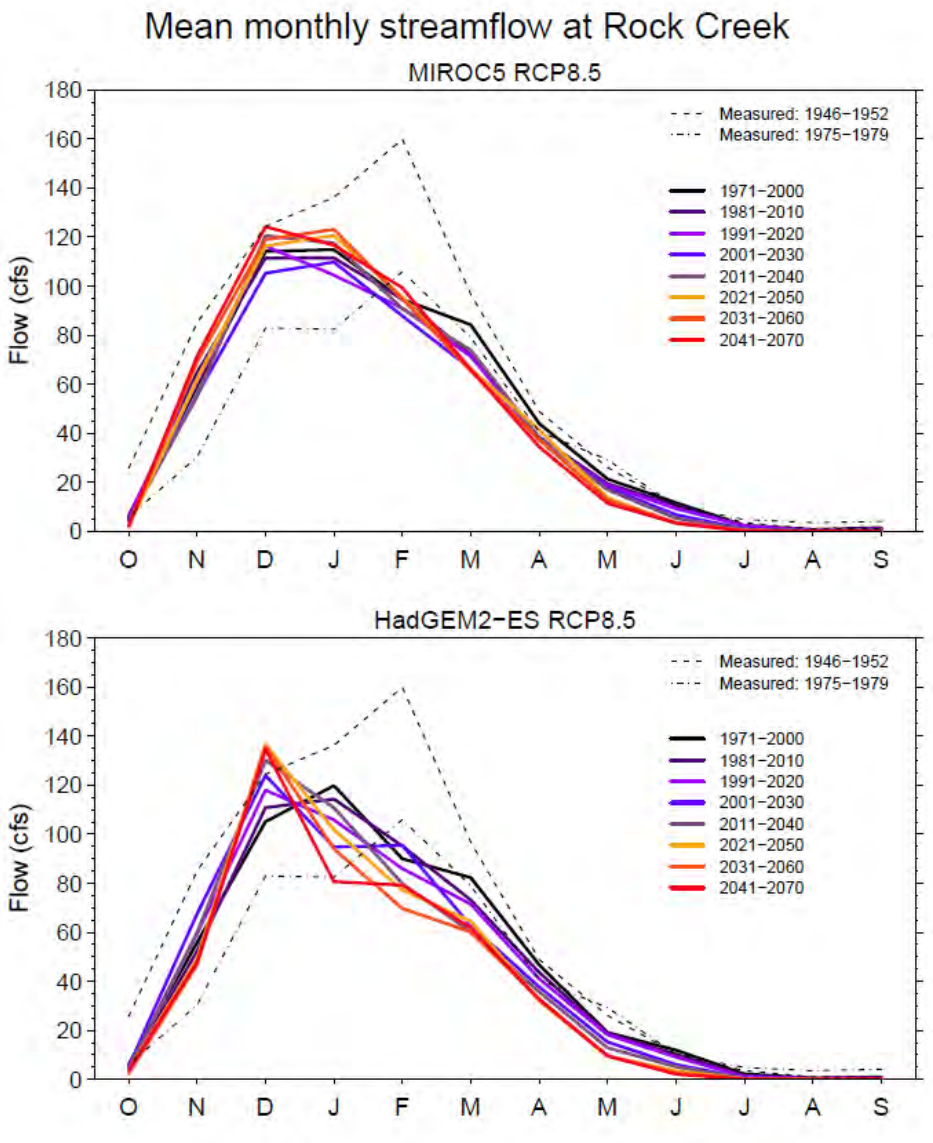

Figure 11. Mean monthly streamflow at Rock Creek from the USGS gauge and from the MIROC5 RCP8.5 (upper panel) and HadGEM2-ES RCP8.5 (lower panel) scenarios. Solid colored lines show simulated streamflow averaged over 30-year periods. Dashed black lines show observed streamflow averaged over to measurement periods (water years 1946-1952 and 1975-1979).

Table 8. Projected relative change (%) in mean monthly streamflow at Rock Creek from 1971-2020 to 2021-2070, averaged over both climate scenarios.

Month	Oct	Nov	Dec	Jan	Feb	Mar	Apr	May	Jun	Jul	Aug	Sep	Annual
Change	-48	-1	+14	-1	-2	-16	-18	-43	-68	-92	-96	-87	-6

Recommendations for Continued Research

Projections of hydroclimatic changes in the Willamette Basin have been generally consistent over multiple studies during the last decade. Today we have the ability to analyze and consider a very large number of seemingly plausible, and often very different, hydrological futures that incorporate natural variability along with uncertainties in future emissions and uncertainties in model accuracy (included modeling of both the future climate response and the hydrological response). This is an important achievement in that it provides a much more complete characterization of our current understanding of what the future may bring in terms of unregulated water supply and flood risk along the mainstem of the Willamette River. In this report, we have treated each of these futures as equally likely. We know this is a poor assumption because some emission scenarios should be more likely than others and some climate and hydrological model are certainly "better" than others, yet correctly assigning different likelihoods to different futures is non-trivial and there is no established best means of doing so. Even so, further research into model accuracy, particular for hydrological models, has the potential for narrowing the wide range in projections by eliminating, or de-emphasizing, those futures that result from what are judged to be poorer models.

For small Coast Range basins such as Rock Creek, the hydrological response to climate change has been much less studied. Projections are limited to a small number of scenarios and the fidelity of both the climate drivers and the hydrological modeling is difficult to assess due to a paucity of meteorological and streamflow measurements. Improvements in the hydrological modeling and simulations using many more scenarios should be done to better characterize the distribution of possible future water supply from Rock Creek.

As of this writing, the state of the science had not matured sufficiently to make reliable projections of the impacts of climate change on water quality in general and HABs in particular. While progress has been made towards understanding the complex pathways that lead to HAB development, what is still needed to assess vulnerabilities in the face of climate change is the translation of this understanding into scale-appropriate and well-tested predictive models that can be used to quantify how HAB frequency and spatial extent might change in Willamette Basin municipal water supplies over the forthcoming decades.

References

Abatzoglou, J. T., Rupp, D. E., & Mote, P. W. (2014a). Seasonal climate variability and change in the Pacific Northwest of the United States. Journal of Climate, 27(5), 2125-2142.

Abatzoglou, J. T., Rupp, D. E., & Mote, P. W. (2014b). Questionable evidence of natural warming of the northwestern United States. Proceedings of the National Academy of Sciences, 111(52), E5605-E5606.

Buccola, N. L., Risley, J. C., & Rounds, S. A. (2016). Simulating future water temperatures in the North Santiam River, Oregon. Journal of Hydrology, 535, 318-330.

Carpenter, K. (2019). Enhanced water-quality monitoring in Detroit Lake and the North Santiam River to support dam operations and drinking water management, 9th Annual North Santiam Basin Summit, May 15, 2019, Salem, OR, May 15, 2019.

Chang, H., & Jung, I. W. (2010). Spatial and temporal changes in runoff caused by climate change in a complex large river basin in Oregon. Journal of Hydrology, 388(3-4), 186-207.

Dalton, M. M., Dello, K. D., Hawkins, L., Mote, P. W., & Rupp, D. E. (2017). The Third Oregon Climate Assessment Report. Oregon Climate Change Research Institute. http://www.occri.net/publications-and-reports/3rd-oregon-climate-assessment-report-2017

Gergel, D. R., Nijssen, B., Abatzoglou, J. T., Lettenmaier, D. P., & Stumbaugh, M. R. (2017). Effects of climate change on snowpack and fire potential in the western USA. Climatic Change, 141(2), 287-299.

Graham, J. L., Dubrovsky, N. M., & Eberts, S. M. (2016). Cyanobacteria Harmful Algal Blooms and US Geological Survey Science Capabilities. Open-File Report 2016–1174, US Department of the Interior, US Geological Survey.

GSI Water Solutions, Inc. (2012). Corvallis Water Management and Conservation Plan, prepared by GSI Water Solutions, Inc., and the Utilities Division of Corvallis Public Works, City of Corvallis, OR.

Huisman, J., & Hulot, F. D. (2005) Population dynamics of harmful cyanobacteria. In: Harmful Cyanobacteria. Aquatic Ecology Series, vol 3. Springer, Dordrecht.

Jaeger, W. K., Amos, A., Bigelow, D. P., Chang, H., Conklin, D. R., Haggerty, R., Langpap, C., Moore, K., Mote, P. W., Nolin, A. W., Plantinga, A. J., Schwartz, C. L., Tullos, D., & Turner, D. P. (2017a). Finding water scarcity amid abundance using human–natural system models. Proceedings of the National Academy of Sciences, 114(45), 11884-11889.

Jaeger, W. K., Plantinga, A., Langpap, C., Bigelow, D., & Moore, K. D. (2017b). Water, economics, and climate change in the Willamette Basin, Oregon. Oregon State University, Extension Service. https://catalog.extension.oregonstate.edu/em9157/html

Jung, I. W., & Chang, H. (2011). Assessment of future runoff trends under multiple climate change scenarios in the Willamette River Basin, Oregon, USA. Hydrological Processes, 25(2), 258-277.

Jung, I. W., & Chang, H. (2012). Climate change impacts on spatial patterns in drought risk in the Willamette River Basin, Oregon, USA. Theoretical and Applied Climatology, 108(3-4), 355-371.

McCabe, G. J., & Wolock, D. M. (2015). Variability and trends in global drought. Earth and Space Science, 2(6), 223-228.

Mote, P.W., Abatzoglou, J., Dello, K. D., Hegewisch, K., & Rupp, D. E. (2019). Fourth Oregon Climate Assessment Report. Oregon Climate Change Research Institute. http://www.occri.net/ocar4.

Oliver, R. L., & Ganf, G. G. (2000). Freshwater blooms. In: The Ecology of Cyanobacteria (pp. 149-194). Springer, Dordrecht.

Rupp, D. E., Abatzoglou, J. T., & Mote, P. W. (2017a). Projections of 21st century climate of the Columbia River Basin. Climate Dynamics, 49(5-6), 1783-1799.

Rupp, D. E., Li, S., Mote, P. W., Shell, K. M., Massey, N., Sparrow, S. N., Wallom, D. C. H., & Allen, M. R. (2017b). Seasonal spatial patterns of projected anthropogenic warming in complex terrain: a modeling study of the western US. Climate dynamics, 48(7-8), 2191-2213.

Schaedel, A. (2011). Oregon DEQ Harmful Algal Bloom (HAB) Strategy. Oregon Department of Environmental Quality.

Tohver, I. M., Hamlet, A. F., & Lee, S. Y. (2014). Impacts of 21st-century climate change on hydrologic extremes in the Pacific Northwest region of North America. JAWRA Journal of the American Water Resources Association, 50(6), 1461-1476.

Van Vuuren, D. P., Edmonds, J., Kainuma, M., Riahi, K., Thomson, A., Hibbard, K., & Masui, T. (2011). The representative concentration pathways: an overview. Climatic Change, 109(1-2), 5.

Vano, J. A., Kim, J. B., Rupp, D. E., & Mote, P. W. (2015). Selecting climate change scenarios using impact-relevant sensitivities. Geophysical Research Letters, 42(13), 5516-5525.

Visser, P. M., Verspagen, J. M., Sandrini, G., Stal, L. J., Matthijs, H. C., Davis, T. W., ... & Huisman, J. (2016). How rising CO_2 and global warming may stimulate harmful cyanobacterial blooms. Harmful Algae, 54, 145-159.

UNFCCC (2015). Paris Agreement. Paper presented at the United Nations Framework Convention on Climate Change. Bonn, Germany.

USGCRP (2016). Chapter 6: Climate impacts on water related illnesses. In: The Impacts of Climate Change on Human Health in the United States: A Scientific Assessment. Crimmins, A., J. Balbus, J.L. Gamble, C.B. Beard, J.E. Bell, D. Dodgen, R.J. Eisen, N. Fann, M.D. Hawkins, S.C. Herring, L. Jantarasami, D.M. Mills, S. Saha, M.C. Sarofim, J. Trtanj, and L. Ziska, Eds. U.S. Global Change Research Program, Washington, DC, 312 pp. http://dx.doi.org/10.7930/J0R49NQX

USGCRP (2017). Chapter 7: Precipitation change in the United States. In: Climate Science Special Report: Fourth National Climate Assessment, Volume I [Wuebbles, D.J., D.W. Fahey, K.A. Hibbard, D.J. Dokken, B.C. Stewart, and T.K. Maycock (eds.)]. U.S. Global Change Research Program, Washington, DC, USA, 470 pp, doi: 10.7930/J0J964J6.

Appendices:

Projected Climate Change Impacts on Water Demand and Supply for the City of Corvallis

Appendix A: Data and methods for water demand metrics

Observed daily precipitation and daily minimum and maximum temperature covering the years 1893-2018 for the Corvallis station located at 44.6341°N, 123.19°W were acquired from the National Centers for Environmental Information (NCEI). The NCEI station identification code is USC00351862 and the station is designated "Corvallis State University, OR US".

Simulated daily precipitation, daily minimum and maximum temperature, and monthly potential evapotranspiration (PET) covering the years 1950-2099 were acquired from the University of Idaho Climatology Lab at http://www.climatologylab.org/maca.html. These simulated meteorological data were derived from global climate model (GCM) output that was statistically downscaled to 1/24 degree (~4 km) spatial resolution over the contiguous United States. The downscaling was done using the Multivariate Adaptive Constructed Analogs Method (MACA; Abatzoglou and Brown, 2012).

The MACA dataset (specifically the version called "MACAv2-METDATA") includes downscaled output from 20 GCMs (see Table A1) that were used in the Coupled-Model Intercomparison Project Phase 5 (CMIP5; Taylor et al., 2012) that provided the climate projections for the International Panel on Climate Change (IPCC) Assessment Report 5 (AR5; IPCC, 2013). This dataset includes climate projections using two scenarios of greenhouse gas and pollutant concentrations described by the Representative Concentration Pathway (RCP) 4.5 and 8.5 (Van Vuuren et al., 2011).

The MACA downscaling process was designed to reproduce realistic spatial patterns of meteorological variables at a daily time step over the continental US; it was not designed to precisely replicate the statistical properties of the meteorological data at any particular station. This means that the MACA data extracted from a grid cell may have biases with respect to station data located in that particular grid cell. In our case, we have extracted the MACA data for the 4x4 km grid cell that contains the location of the Corvallis station and assume the data for that grid cell is representative of Corvallis.

Table A1. Global climate models[1] included in this report.	
bcc-csm1-1	HadGEM2-ES
bcc-csm1-1-m	inmcm4
BNU-ESM	IPSL-CM5A-LR
CanESM2	IPSL-CM5A-MR
CCSM4	IPSL-CM5B-LR
CNRM-CM5	MIROC-ESM
CSIRO-Mk3-6-0	MIROC-ESM-CHEM
GFDL-ESM2G	MIROC5
GFDL-ESM2M	MRI-CGCM3
HadGEM2-CC365	NorESM1-M
[1]The CMIP5 initial conditions ensemble member r1i1p1 was used from each GCM, except for CCSM4 (r6i1p1).	

Because of discrepancies between the MACA and station data, we implemented a bias-correction step to adjust the MACA temperature and precipitation to be statistically consistent with the Corvallis station data. A quantile mapping procedure was applied in R (Gudmundsson, 2016; R Core Team, 2018) so that the frequency distributions of daily minimum and maximum temperature and daily precipitation over the years 1950-2005 were similar between the MACA and Corvallis station data.

PET was calculated on a monthly time step using the Penman-Monteith-based FAO reference crop potential evapotranspiration from a well-watered soil (Allen et al., 1998). The monthly meteorological variables required in the calculation came directly from the MACA datasets (temperature, specific humidity, wind speed, and downward short-wave radiation) or were derived from the MACA data (e.g., cloud cover and downward long-wave radiation; see http://www.fao.org/3/X0490E/x0490e07.htm#concepts). No additional bias-correction was done to PET so it inherits any biases that may exist in the input variables. It is important to note that the PET calculations assume no changes in water use efficiency of vegetation in response to increasing CO_2 concentrations in the atmosphere. How vegetation will respond to increasing CO_2 in the short and long-term is uncertain, but it is expected that water use efficiency would increase, at least in the short-term, as plants require less transpiration to acquire the same amount of carbon under higher CO_2 concentrations. The projected increases in PET projections given here, therefore, may be overestimated.

Appendix B: Data and methods for water supply metrics

Willamette River

The USACE has estimated what the streamflow would have been at many locations along the Willamette River and its major tributaries had there been no reservoir operations nor water used for irrigation (i.e., no-regulation, no-irrigation, or "NRNI", streamflow). Daily NRNI streamflow for Albany and Salem for the years 1928-2008 were downloaded from https://www.bpa.gov/p/Power-Products/Historical-Streamflow-Data/Pages/No-Regulation-No-Irrigation-Data.aspx. NRNI flows for Corvallis are not available so this analysis considers flows at Albany and Salem instead. It is reasonable to assume that relative changes in flow conditions at Corvallis will be similar to relative changes in flow conditions at Albany.

To compare with the historical NRNI flows, actual observed daily streamflow on the Willamette River at Albany (USGS 14174000) and Salem (USGS 14191000) were downloaded from the USGS at https://waterdata.usgs.gov/nwis/inventory/?site_no=14174000, and https://waterdata.usgs.gov/nwis/inventory/?site_no=14191000 and, respectively.

Future projections of 'NRNI-type' daily streamflow have recently been generated under a project funded by the Bonneville Power Administration, USACE, and Bureau of Reclamation (RMJOC, 2018). This project is referred to here as the Columbia River Climate Change (CRCC) project. These simulations span the years 1950-2099 and were generated using 160 distinct modeling configurations (thus there are 160 time series per location). The 160 configurations are the product of 4 hydrological model variants driven with inputs derived from 10 global climate models (GCMs) forced with 2 greenhouse gas (GHG) concentration scenarios. Daily temperature and precipitation from the GCM simulations were downscaled using 2 methods.

The post-2005 GHG scenarios are the Representative Concentration Pathways (RCPs) 4.5 and 8.5 (see discussion in Appendix A); historical GHG concentrations were used prior to 2006. The GCM output are from CMIP5 and the following GCMs were chosen based on relatively good performance with regards to observed historical climate (Rupp et al., 2013) and availability of the MACA-downscaled data: CanESM2, CCSM4, CNRM-CM5, CSIRO-Mk3-6-0, GFDL-ESM2M, HadGEM2-CC, HadGEM2-ES, Inmcm4, IPSL-CM5A-MR, MIROC5. These 10 GCMs are a subset of those listed in Table A1. The CMIP5 initial conditions ensemble member r1i1p1 was used from each GCM, except for CCSM4 (r6i1p1). The GCM data were statistically downscaled to 1/16 degree spatial resolution using two methods: 1) Multivariate Adaptive Constructed Analogs method (MACAv2-Livneh; Abatzoglou and Brown, 2012) and the Bias Correction Spatial Disaggregation method (BCSD; Wood et al., 2004).

The 4 hydrological model variants (simply referred to as distinct 'models' hereafter) consist of three implementations of the Variable Infiltration Capacity Model (VIC; Liang et al., 1994) and a gridded implementation of the Precipitation-Runoff Modeling System (PRMS; Leavesley et al., 1983), all at 1/16 degree (~6 km). The three VIC implementations vary by the calibration method; they are referred to as VIC-P1, VIC-P2, and VIC-P3. PRMS (PRMS-P1) was calibrated similarly to VIC-P1. See Chegwidden et al. (2019) for an overview of the CRCC simulations, including a discussion of the calibration methods and streamflow network routing scheme.

Simulated streamflow was bias-corrected against estimated historical NRNI flows at selected locations to reduce biases that existed despite model calibration (RMJOC, 2018). The streamflow data for the Willamette at Albany and Salem were downloaded from the University of Washington at http://www.hydro.washington.edu/CRCC/.

Streamflow projections for two future scenarios were also acquired from the Willamette Water 2100 project (WW2100; Jaeger et al., 2017a; 2017b). The climate data used in these projections are based on RCP8.5 scenario and are similar to those used for CRCC but are limited to two GCMs: HadGEM2-ES and MIROC5.

WW2100 used the hydrological model (the Hydrologiska Byråns Vattenbalansavdelning, or 'HBV' model adapted for the WW2100 model framework; Jaeger et al., 2017a), which is different from any of the models used in CRCC. Also unlike the CRCC projections, the WW2100 projections simulate the effects of the reservoirs, agriculture and municipal water use, and water rights. Built into these projections are assumptions about population growth, land use change, changes in water pricing, improvements in water use efficiency, etc.

Daily flows for the Willamette River at Salem were acquired from the WW2100 database; flows at Albany or Corvallis were not archived as part of WW2100. WW2100 data are accessible here: https://inr.oregonstate.edu/ww2100/data-simulations/downloads.

Flood frequency statistics were based on the annual water year (Oct. 1 – Sep. 30) daily maximum streamflow in the Willamette River at Albany. Following Lind and Stonewall (2018), a log-Pearson type III (LP3) probability distribution was fitted to both the NRNI and CRCC streamflow data. From the LP3 distribution, the annual maximum streamflows with a 4%, 1%, and 0.2% probability of being exceeded were estimated. The streamflow records were split into two periods: Water years 1951-2000 and 2021-2070. Flood frequency statistics were estimated separately for each period.

Potential threat to future water supply during periods of low streamflow was quantified by calculating number of days per year and per month that streamflow dropped below the threshold values 2,285 cfs at Albany and 2,150 cfs at Salem. These values were calculated from all the observed and simulated streamflow time series.

Rock Creek

Observed daily streamflow at Rock Creek near Philomath, OR (USGS 14170500) were downloaded from the USGS at https://waterdata.usgs.gov/or/nwis/dv?referred_module=sw&site_no=14170500. These data only span the water years 1946-1952 and 1975-1979.

Because streamflow projections for Rock Creek were not archived as part of the WW2100, the same two future climate scenarios used in WW2100 were simulated using an updated version of the WW2100 model: the Community Willamette Whole Watershed Model (CW3M; Dave Conklin, Oregon Freshwater Simulations, personal communication). Daily streamflow at Rock Creek was simulated for the years 1970 to 2070.

30-year and 50-year long-term monthly means were calculated from the daily streamflow values. Extreme low- and high-flow statistics were not calculated because the quality of the simulations was not deemed high enough to do such an analysis.

References

Abatzoglou, J. T., & Brown, T. J. (2012). A comparison of statistical downscaling methods suited for wildfire applications. International Journal of Climatology, 32(5), 772-780.

Allen, R. G., Pereira, L. S., Raes, D., & Smith, M. (1998). Crop evapotranspiration-Guidelines for computing crop water requirements-FAO Irrigation and drainage paper 56. FAO, Rome, 300(9), D05109.

Chegwidden, O. S., Nijssen, B., Rupp, D. E., Arnold, J. R., Clark, M. P., Hamman, J. J., ... & Pan, M. (2019). How do modeling decisions affect the spread among hydrologic climate change projections? Exploring a large ensemble of simulations across a diversity of hydroclimates. Earth's Future, 7(6), 623-637.

Gudmundsson, L. (2016). qmap: Statistical transformations for post-processing climate model output. R package version 1.0-4.

IPCC (2013). Climate Change 2013: The Physical Science Basis. Contribution of Working Group I to the Fifth Assessment Report of the Intergovernmental Panel on Climate Change [Stocker, T.F., et al. (eds.)]. Cambridge University Press, Cambridge, United Kingdom and New York, NY, USA, 1535 pp.

Jaeger, W. K., Amos, A., Bigelow, D. P., Chang, H., Conklin, D. R., Haggerty, R., Langpap, C., Moore, K., Mote, P. W., Nolin, A. W., Plantinga, A. J., Schwartz, C. L., Tullos, D., & Turner, D. P. (2017a). Finding water scarcity amid abundance using human–natural system models. Proceedings of the National Academy of Sciences, 114(45), 11884-11889

Jaeger, W. K., Plantinga, A., Langpap, C., Bigelow, D., & Moore, K. D. (2017b). Water, economics, and climate change in the Willamette Basin, Oregon. Oregon State University, Extension Service. https://catalog.extension.oregonstate.edu/em9157/html

Leavesley, G. H., Lichty, R. W., Troutman, B. M., & Saindon, L. G. (1983). Precipitation-runoff modeling system - User's manual, U.S. Geological Survey Water-Resources Investigations Report, 83(4238), 207.

Liang, X., Lettenmaier, D. P., Wood, E. F., & Burges, S. J. (1994). A simple hydrologically based model of land surface water and energy fluxes for general circulation models. Journal of Geophysical Research: Atmospheres, 99(D7), 14415–14428. https://doi.org/10.1029/94JD00483

Lind, G. D., & Stonewall, A. J. (2018). Preliminary flood-duration frequency estimates using naturalized streamflow records for the Willamette River Basin, Oregon (No. 2018-1020). US Geological Survey.

R Core Team (2018). R: A language and environment for statistical computing. R Foundation for Statistical Computing, Vienna, Austria. URL https://www.R-project.org/.

River Management Joint Operating Committee (RMJOC) (2018). Climate and Hydrology Datasets for RMJOC Long-Term Planning Studies, Second Edition: Part 1 – Hydroclimate Projections and Analyses. Retrieved from https://www.bpa.gov/p/Generation/Hydro/Pages/Climate-670 Change-FCRPS-Hydro.aspx.

Rupp, D. E., Abatzoglou, J. T., Hegewisch, K. C., & Mote, P. W. (2013). Evaluation of CMIP5 20th century climate simulations for the Pacific Northwest USA. Journal of Geophysical Research: Atmospheres, 118(19), 10884-10906. https://doi.org/10.1002/jgrd.50843

Taylor, K. E., Stouffer, R. J., & Meehl, G. A. (2012). An overview of CMIP5 and the experiment design. Bulletin of the American Meteorological Society, 93(4), 485–498. https://doi.org/10.1175/BAMS-D-11-00094.1

Van Vuuren, D. P., Edmonds, J., Kainuma, M., Riahi, K., Thomson, A., Hibbard, K., & Masui, T. (2011). The representative concentration pathways: an overview. Climatic Change, 109(1-2), 5.

Wood, A. W., Leung, L. R., Sridhar, V., & Lettenmaier, D. P. (2004). Hydrologic implications of dynamical and statistical approaches to downscaling climate model outputs. Climatic Change, 62(1–3), 189–2